

Neutron Charge Density from Simple Pion Cloud Models

Jared A. Rinehimer and Gerald A. Miller

Department of Physics, University of Washington,

Seattle, Washington 98195-1560, USA

(Dated: June 26, 2009)

Abstract

The physical nucleon is modeled as a bare nucleon surrounded by a pion cloud using a pseudoscalar pion-nucleon coupling to examine its implications for the neutron form factor, $F_1(Q^2)$, and the corresponding transverse charge density, $\rho(b)$ in the infinite momentum frame. Two versions, one with a tunable Pauli-Villars parameter, and one with light-front cloudy-bag pion-nucleon form factors, are examined. A qualitative agreement with the experimental form factor ($F_1 < 0$ for all Q^2) and transverse charge density are achieved when the nucleon is treated as having a finite extent. The bare nucleon must have a finite extent if this model is to account for a negative definite F_1 , and consequently a negative transverse charge density of the neutron at its center.

PACS numbers: 14.20.Dh, 13.40.Gp

INTRODUCTION

It has been recently demonstrated that the neutron transverse charge density is negative at the center [1]. This surprising result seems to contrast with many long-standing arguments such as the 1947 predictions provided Fermi and Marshall, meson cloud models, and arguments from gluon exchange [2, 3, 4, 5, 6]. As such, this discovery requires new attempts at understanding the physics behind the currently observed transverse density. This paper seeks to use specific toy models to predict a qualitatively similar structure in order to shed light on the physics involved.

The nucleonic form factors are defined by the matrix element of the electromagnetic current operator $J^\mu(x)$ as

$$\langle p', \lambda' | J^\mu(0) | p, \lambda \rangle = \bar{u}(p', \lambda') [\gamma^\mu F_1(Q^2) + i \frac{\sigma^{\mu\nu} q_\nu}{2M} F_2(Q^2)] u(p, \lambda), \quad (1)$$

where $q = p' - p$ is the momentum transfer which is space-like such that $0 < -q^2 \equiv Q^2$. These form factors have the common interpretation of being related to the charge and magnetization density of the nucleon in question, however such an interpretation is only valid at zero momentum transfer for which the initial and final nucleon wave functions are the same. In the infinite momentum frame (IMF), however, the transverse charge density has been shown to be the two dimensional Fourier transform of the form factor $F_1(Q^2)$ [1, 7, 8, 9, 10]. Production of these form factors in a model will have implications for the physics involved with the negative transverse charge density of the neutron.

MODELS

In this paper, we model the physical nucleon as a bare nucleon surrounded by a pion cloud using pseudoscalar pion-nucleon coupling [11], starting with the bare nucleon assumed to be a point particle. To one-loop order, two diagrams exist for the interaction of the neutron with a virtual photon, as shown in Fig. 1.

Model 1

For the first model, we introduce a Pauli-Villars regulator on the pion, with the result that in the calculation of each diagram, one subtracts a term identical to the diagram with

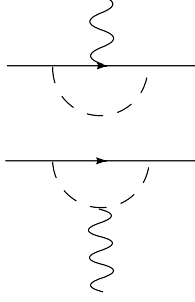


FIG. 1: The two diagrams for the neutron-photon interaction to one loop order. The dashed lines represent pion propagators, the solid represent nucleon propagators.

the exception of the pion mass being replaced by the regulator mass Λ . This regulator is then used as a tunable parameter for the theory, with the advantage that this procedure is co-variant and does not alter the Ward identities. The first diagram in Fig. 1, evaluates to

$$\left(4eg_0^2 \bar{u}(p') \int dx dy dz \frac{d^4 \ell}{(2\pi)^4} \delta(1-x-y-z) \left[\frac{\ell^2/2 - (x+y)^2 M^2 + xyQ^2}{(\ell^2 - \Delta_{m_\pi})^3} \gamma^\mu + \frac{2M^2(x+y)^2}{(\ell^2 - \Delta_{m_\pi})^3} \frac{i\sigma^{\mu\nu}}{2M} q_\nu \right] u(p) \right) - (m_\pi \leftrightarrow \Lambda) \quad (2)$$

where

$$\Delta_{m_\pi} = z m_\pi^2 + (x+y)^2 M^2 + xyQ^2, \quad (3)$$

and ϵ_μ^* is the polarization of the virtual photon and is omitted for the calculation of the matrix elements of $J^\mu(0)$, p is the incoming 4-momentum, p' is the outgoing 4-momentum, M is the neutron mass and m_π is the pion mass(π^-). The second diagram is

$$\left(4eg_0^2 \bar{u}(p') \int dx dy dz \frac{d^4 \ell}{(2\pi)^4} \delta(1-x-y-z) \left[\frac{-\ell^2/2 - 2M^2 z^2}{(\ell^2 - \Delta'_{m_\pi})^3} \gamma^\mu + \frac{2M^2 z^2}{(\ell^2 - \Delta'_{m_\pi})^3} \frac{i\sigma^{\mu\nu}}{2M} q_\nu \right] u(p) \right) - (m_\pi \leftrightarrow \Lambda) \quad (4)$$

where

$$\Delta'_{m_\pi} = M^2 z^2 + (x+y)m_\pi^2 + xyQ^2. \quad (5)$$

By examining (1), the terms proportional to γ^μ correspond to F_1 , while the terms proportional to $\frac{i\sigma^{\mu\nu}}{2M} q_\nu$ correspond to F_2 . We can evaluate the integral over the loop momentum ℓ by Wick rotation, and the divergent terms cancel due to the Pauli-Villars procedure. Then, we must sum both diagrams together for the full contribution, giving expressions for the

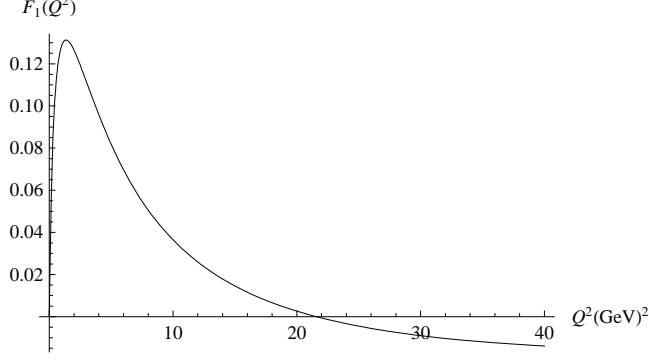


FIG. 2: The form factor $F_1(Q^2)$ for the Pauli-Villars model, with $\Lambda = 1.0$ GeV. It is important to note that $F_1 > 0$ for some values of Q^2 , while the observed $F_1(Q^2)$ is negative for all Q^2 .

form factors

$$\begin{aligned}
F_1(Q^2) = & \frac{g_0^2}{8\pi^2} \int_0^1 \int_0^{1-x} dx dy \left[\ln \left(\frac{\Delta_\Lambda \Delta'_{m_\pi}}{\Delta_{m_\pi} \Delta'_\Lambda} \right) \right. \\
& + \left((x+y)^2 M^2 - xy Q^2 \right) \left(\frac{1}{\Delta_{m_\pi}} - \frac{1}{\Delta_\Lambda} \right) \\
& \left. + 2M^2(1-x-y)^2 \left(\frac{1}{\Delta'_{m_\pi}} - \frac{1}{\Delta'_\Lambda} \right) \right], \tag{6}
\end{aligned}$$

and,

$$F_2(Q^2) = -M^2 \frac{g_0^2}{4\pi^2} \int_0^1 \int_0^{1-x} dx dy \left[(x+y)^2 \left(\frac{1}{\Delta_{m_\pi}} - \frac{1}{\Delta_\Lambda} \right) + (1-x-y)^2 \left(\frac{1}{\Delta'_{m_\pi}} - \frac{1}{\Delta'_\Lambda} \right) \right] \tag{7}$$

Numerical integration over Feynman parameters yields a functional form for $F_1(Q^2)$ and $F_2(Q^2)$, which is used to derive a numerical interpolating function. We use a neutron mass of $M = 0.93957$ GeV and pion mass of $m_\pi = 0.13957$ GeV with a coupling of $\frac{g_0^2}{4\pi} = 13.5$. The value of $\Lambda = 1.0$ GeV is selected since it yields $F_2(0) = -1.9091$, close to the expected magnetic moment of the neutron. Also numerical integration verifies that $F_1(0) = 0$, which agrees with charge conservation. A plot of $F_1(Q^2)$ appears in Fig 2.

As stated before, the two-dimensional Fourier transform of F_1 is the charge density in the IMF. Since F_1 lacks angular dependence, this density becomes

$$\rho(b) = \int \frac{Q dQ}{2\pi} F_1(Q^2) J_0(bQ). \tag{8}$$

where J_0 is a Bessel function of the first kind, b is the transverse distance from the origin. Using the interpolation function $F_1(Q^2)$, we find the charge density by integrating to a

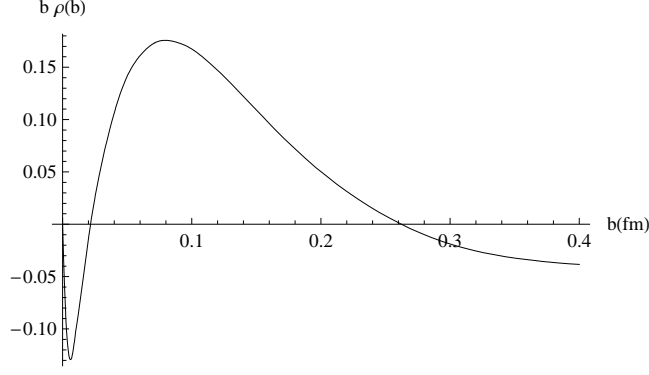


FIG. 3: The transverse charge density in the infinite momentum frame, derived from the form factor from Fig. 2.

sufficiently high cutoff. A plot of this charge density appears in Fig. 3. The density is negative at the center ($b = 0$), becomes positive as the value of b increases, and then at still larger values of b has a long, negative tail as found in [1]. This indicates in this model that the pion wave-function possesses some non-zero probability to exist at the center of the neutron, since the only negatively charged constituent of each Feynman diagram is the π^- . This model however, yields a form factor for the neutron that disagrees with observed data. In particular, $F_1 > 0$ for some values of Q^2 , while the observed F_1 is negative definite.

Model 2

Another procedure is to calculate the diagrams by using a distinct form factor at each pion-nucleon vertex. Then we use the light-front coordinates and an integration over the k^- variable to find numerically integrable expressions for the form factor contributions from each Feynman diagram in Fig. 1. The first diagram in Fig. 1 gives a term contributing to $F_1(Q^2)$ of the neutron as

$$F_{n1,1}(Q^2) = g_0^2 \int_0^1 dx \int \frac{d^2 L}{(2\pi)^3} R(\mathbf{L}_+^2, x) R(\mathbf{L}_-^2, x) (x^2(M^2 - Q^2/4) + \mathbf{L}^2) \quad (9)$$

while the second diagram gives

$$F_{n1,2}(Q^2) = -g_0^2 \int_0^1 dx \int \frac{d^2 K}{(2\pi)^3} R(\mathbf{K}_+^2, x) R(\mathbf{K}_-^2, x) (\mathbf{K}^2 + M^2 x^2 - (1-x)^2 Q^2/4) \quad (10)$$

where \mathbf{L} is a shifted transverse momentum integration parameter in the light-front coordinates, $\mathbf{L}_\pm = \mathbf{L} \pm x\mathbf{q}/2$, $x = k^+/p^+$, k^μ is the virtual pion momentum, $R(k^2, x) =$

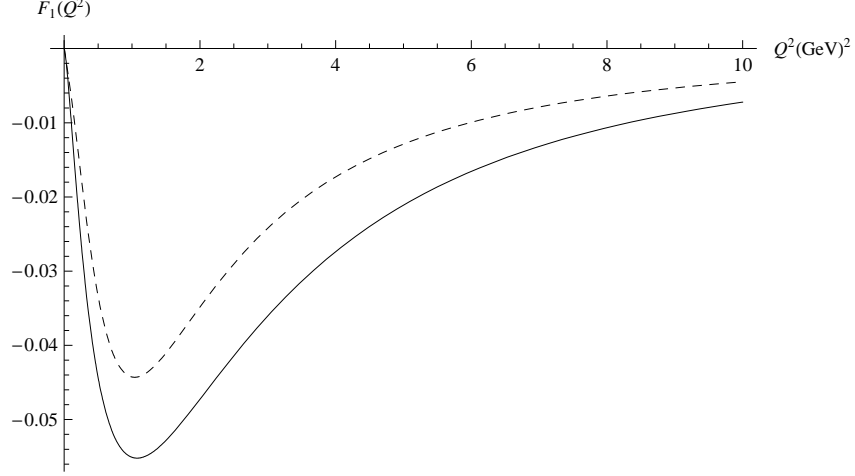


FIG. 4: Solid: The form factor F_1 for the neutron, using the value $r_s^2 = 10(\text{GeV})^{-2} \approx 0.39\text{fm}^2$. Dashed: The parametrization of [16].

$F_{\pi N}(\mathbf{k}_\perp^2, x)/D(\mathbf{k}_\perp^2, x)$, $D(\mathbf{k}_\perp^2, x) = M^2x^2 + \mathbf{k}_\perp^2 + m_\pi^2(1-x)$, and the nucleon-pion form factor $F_{\pi N}$ is given by [12, 13, 14, 15]

$$F_{\pi N}(\mathbf{k}_\perp^2, x) = e^{-D(\mathbf{k}_\perp^2, x)/2x(1-x)\Lambda'}.$$
 (11)

Finally, on the first term of F_{1n} for the neutron,(9), we multiply by a factor

$$\chi = \frac{1}{(1 + Q^2 r_s^2/12)^2},$$
 (12)

where r_s is a free radius parameter. This factor corresponds to granting an extent to the bare proton in the first diagram of Fig. 1. Without this introduction, the form factor would be positive for some small values of Q^2 , which does not agree with observation. The expression for the form factors are then numerically integrated over \mathbf{L}^2 and x to give the behavior versus Q^2 only. The final expression yields a form factor F_{1n} for the neutron that is qualitatively similar to that of existing parameterizations [16, 17]. The form factor with $r_s^2 = 10.0 \text{ GeV}^{-2} \approx 0.39 \text{ fm}^2$, $\Lambda = 1.25 \text{ GeV}$, $g_0^2/4\pi = 13.5$, and the parameterization from [16] appear in Fig. 4. The corresponding transverse charge density, the two-dimensional Fourier transform of this version of F_1 , is obtained from Eq. (8), and appears in Fig. 5. The transverse charge density from Model 2 qualitatively agrees with the current observation that $\rho(b)$ is negative at the center, is positive in the middle and negative at the far edge.

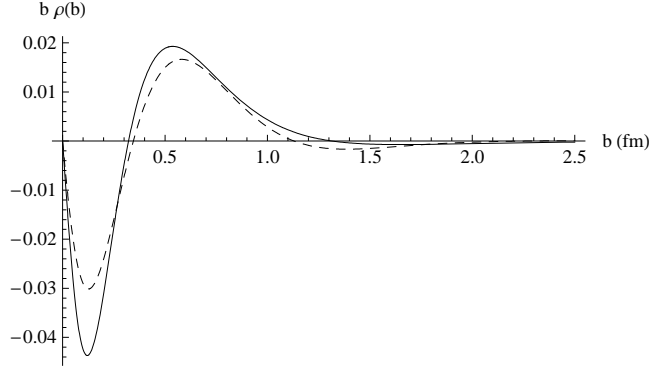


FIG. 5: Solid: The transverse charge density for the form factor from Fig. 4. Dashed: The transverse charge density for the parametrization of [16].

SUMMARY

The form factor for Model 2 agrees with the observation that the measured form factor is negative for all values of Q^2 . Achieving this occurs only with the insertion of a term that accounts for the finite spatial extension of the bare nucleon. Without the introduction of the factor (12), the F_1 function and the transverse charge density $\rho(b)$ look qualitatively similar to that of Fig. 2 and Fig. 3, respectively. Thus accounting for the finite extension of the bare nucleon is necessary to achieve a qualitatively reasonable treatment of the neutron's F_1 within the present framework.

The present model is not realistic because the factor (12) is not computed from an underlying model and because proton properties are not studied. Future work will be concerned with obtaining a better, more rigorous formalism that outlines possible physical justifications for the observed transverse charge distribution within the neutron.

Acknowledgments

We thank the USDOE for partial support of this work.

-
- [1] G. A. Miller, Phys. Rev. Lett. **99**, 112001 (2007).
 - [2] E. Fermi and L. Marshall, Phys. Rev. **72**, 1146 (1947).
 - [3] A. W. Thomas, S. Théberge, and G. A. Miller, Phys. Rev. D **24**, 216 (1981).

- [4] J. L. Friar, Part. Nucl. **4**, 153 (1972).
- [5] R. D. Carlitz, S. D. Ellis, and R. Savit, Phys. Lett. B **68**, 443 (1977).
- [6] N. Isgur, G. Karl, and D. W. L. Sprung, Phys. Rev. D **23**, 163 (1981).
- [7] D. E. Soper, Phys. Rev. **D15**, 1141 (1977).
- [8] M. Burkardt, Int. J. Mod. Phys. **A18**, 173 (2003), hep-ph/0207047.
- [9] M. Diehl, Eur. Phys. J. **C25**, 223 (2002), hep-ph/0205208.
- [10] C. E. Carlson and M. Vanderhaeghen, Phys. Rev. Lett. **100**, 032004 (2008), 0710.0835.
- [11] J. D. Bjorken and S. D. Drell, *Relativistic Quantum Mechanics* (McGraw Hill, 1964).
- [12] V. R. Zoller, Z. Phys C **53**, 443 (1992).
- [13] H. Holtmann, A. Szczurek, and J. Speth, Nucl. Phys. A **A596**, 631 (1996).
- [14] G. A. Miller, Phys. Rev. **C66**, 032201 (2002), nucl-th/0207007.
- [15] H. H. Matevosyan, G. A. Miller, and A. W. Thomas, Phys. Rev. C **71**, 055204 (2005).
- [16] J. J. Kelly, Phys. Rev. C **70**, 068202 (2004).
- [17] R. Bradford, A. Bodek, H. Budd, and J. Arrington, Nucl. Phys. B **159**, 127 (2006).